

# DeepFake: Deep Dueling-based Deception Strategy to Defeat Reactive Jammers

Nguyen Van Huynh, Dinh Thai Hoang, Diep N. Nguyen, and Eryk Dutkiewicz

## Abstract

In this paper, we introduce DeepFake, a novel deep reinforcement learning-based deception strategy to deal with reactive jamming attacks. In particular, for a smart and reactive jamming attack, the jammer is able to sense the channel and attack the channel if it detects communications from the legitimate transmitter. To deal with such attacks, we propose an intelligent deception strategy which allows the legitimate transmitter to transmit “fake” signals to attract the jammer. Then, if the jammer attacks the channel, the transmitter can leverage the strong jamming signals to transmit data by using ambient backscatter communication technology or harvest energy from the strong jamming signals for future use. By doing so, we can not only undermine the attack ability of the jammer, but also utilize jamming signals to improve the system performance. To effectively learn from and adapt to the dynamic and uncertainty of jamming attacks, we develop a novel deep reinforcement learning algorithm using the deep dueling neural network architecture to obtain the optimal policy with thousand times faster than those of the conventional reinforcement algorithms. Extensive simulation results reveal that our proposed DeepFake framework is superior to other anti-jamming strategies in terms of throughput, packet loss, and learning rate.

## Index Terms

Anti-jamming, reactive jammer, deception mechanism, ambient backscatter, RF energy harvesting, deep dueling, deep Q-learning, deep reinforcement learning.

## I. INTRODUCTION

Due to the open and broadcast nature of wireless links, wireless communications are extremely vulnerable to jamming attacks, especially for low-power systems such as Internet of Things (IoT). In practice, the jammers can easily launch attacks by injecting high-power interference to the target communication channel [1]. Consequently, the signal-to-interference-plus-noise ratio (SINR) at the receiver can be significantly reduced, and thus the receiver may not be able to

Nguyen Van Huynh, Dinh Thai Hoang, Diep N. Nguyen, and Eryk Dutkiewicz are with University of Technology Sydney, Australia. E-mails: [huynh.nguyenvan@student.uts.edu.au](mailto:huynh.nguyenvan@student.uts.edu.au), [{Hoang.Dinh, Diep.Nguyen, and Eryk.Dutkiewicz}@uts.edu.au](mailto:{Hoang.Dinh, Diep.Nguyen, and Eryk.Dutkiewicz}@uts.edu.au).

decode the information sent from the transmitter. Among radio jamming methods, dealing with reactive jamming is very challenging as the jammer can “smartly” attack the channel whenever it detects transmissions from the transmitter on the channel. In addition, detecting reactive jammer is more difficult as the detector might not be able to distinguish between the jamming signals and the signals sent from the transmitter. More importantly, reactive jamming can be easily launched by conventional jammers by equipping off-the-shelf signal-detection circuits. Thus, reactive jamming attacks can cause serious consequences in critical communications systems such as military, medical, and public safety. As such, defending reactive jamming attacks has been an urgent mission for future wireless communication networks.

#### *A. Current Solutions and Limitations*

Various anti-jamming solutions have been proposed in the literature. Nevertheless, these solutions are not effective in dealing with reactive jammers. In this section, we will study existing anti-jamming solutions together with their limitations in dealing with reactive jamming attacks.

*1) Regulating Transmit Power:* Regulating the transmit power at the legitimate transmitter is the simplest solution and was introduced from the early days of dealing with jamming attacks [2]. In particular, a transmitter can choose to transmit at a very low power level so that the jammer cannot detect its transmission. However, in this way, the jammer can always force the transmitter to transmit data at a very low rate, and the transmitter even cannot transmit data if the jammer is equipped with a very sensitive signal-detection circuit. Another solution for the transmitter is transmitting signals at a very high power level to dominate jamming signals. Nevertheless, this solution possesses several drawbacks. First, increasing the transmit power introduces a new problem as the transmitter can cause unintentional interference to other nearby radio systems [3]. Second, with reactive jammers which can sense the legitimate transmissions and adjust its attack strategy, e.g., increase the attack power level, transmitting signals at high power levels is not an effective way. Finally, if the jammer has a sufficient power budget, it can always disrupt all the ongoing transmissions.

*2) Frequency Hopping:* Frequency-hopping spread spectrum (FHSS) is a common technology when dealing with jamming attacks [4]-[7]. The key idea of this technique is using a switching algorithm that allows the transmitter and receiver to find a new channel for communications once the current channel is attacked by the jammer. In [4], the authors introduced an integrated bit-level FHSS transmitter to mitigate jamming attacks for low-power wireless communication systems. The key idea of the proposed transmitter is exploiting the frequency agility of bulk acoustic wave resonators. In [7], the authors proposed a hybrid approach to cope with fast-following jammers.

To do that, FHSS and direct sequence spread spectrum (DSSS) are deployed with 55 frequency channels in which each channel implements the DSSS modulation with a 16-bit Pseudo noise code. Differently, the authors in [8] aimed to avoid jamming attacks by introducing a stochastic game framework. Through the minimax-Q learning algorithm, the transmitter is able to gradually obtain the optimal defense policy, i.e., how to switch between different channels. Similarly, a game theory based anti-jamming framework for frequency hopping wireless communications was introduced in [9] and [10].

Nevertheless, these solutions and others in the literature possess several limitations in dealing with reactive jamming attacks. First, when the transmitter hops to a new channel, the reactive jammer also can discern/sense the transmitter's activities to attack the new channel. Second, the FHSS schemes require multiple available channels for communications at the same time and a predefined switching algorithm implemented on both the transmitter and receiver. As such, this solution may not be feasible to widely implement on resource-constrained and channel-limited wireless systems. More importantly, if the jammers have sufficient energy to attack all the channels simultaneously, the FHSS schemes do not work anymore. In addition, the game models proposed in [8], [9], and [10] may not be effective as they require complete information of the jammer, which may not be available in advance in practice especially when dealing with the reactive jammer which can adjust its attack strategy by sensing the transmitter's transmissions.

*3) Rate Adaptation:* Another countermeasure to prevent and mitigate impacts of jamming attacks is the rate adaptation (RA) technique [11]-[14]. The key principle of the RA technique is that the transmitter can reduce its data rate under jamming attacks. In particular, under jamming attacks, the channel condition is not good with interference from the jammer. Thus, reducing the data rate is a potential solution as a lower rate is more reliable and suitable for poor channel quality [14]. However, this technique possesses several limitations. The authors in [14] and [12] demonstrated that the RA technique is not effective on a single channel and in dealing with reactive jamming attacks. In particular, this technique assumes that the transmitter can observe the actual jammer's attack performance before selecting an appropriate transmission rate at which the receiver can successfully decode the information. However, for reactive jammers, they only attack the channels after the transmitter transmits data, and thus the RA technique is not effective in dealing with the reactive jammers.

*4) Recent Solutions:* Recently, there are some new ideas introduced to deal with jamming attacks which are especially efficient for low-power systems. Specifically, the authors in [16] proposed the idea of harvesting energy from jamming signals. This is stemmed from the fact that the jammers usually use high transmission power levels to disturb legitimate communications,

and thus the limited-energy devices (e.g., IoT devices) can harvest an abundant energy from the jammers by using RF energy harvesting techniques. In [17], the authors introduced a new approach of using ambient backscatter technology [20] to deal with jamming attacks. The key idea of this approach is that when the jammer attacks the channel, the transmitter can backscatter the jamming signals to transmit data to the receiver. With these solutions, the transmitter does not need to “hide” or “escape” from the jammer as it can leverage the strong jamming signals for its transmissions. As such, the more power the jammer uses to attack the channel, the more benefit, e.g., harvested energy and throughput, the transmitter can achieve. However, for these solutions, they only work well with proactive jammers because the transmitter only can harvest energy or backscatter from jamming signals after the jammers attack the channel. For reactive jammers, they will not attack if there is no activities of the transmitter on the channel, and thus these solutions are not applicable to defeat the reactive jammers. Given the above, dealing with reactive jammers is very challenging, especially for low-power communication systems and when the jammer’s power budget is high. To the best of our knowledge, all current anti-jamming approaches cannot efficiently deal with reactive jamming attacks.

### *B. Main Contributions*

In this paper, we develop an intelligent anti-jamming framework to cope with a powerful reactive jammer which can attack the channel once it detects active transmissions from the transmitter. In particular, we first introduce a deception mechanism that allows the transmitter to lure the jammer by actively transmitting signals for a short period of time. After that, if the jammer attacks the channel, we propose the ideas that allow the transmitter to either harvest energy from the jamming signal, backscatter jamming signals to transmit data using ambient backscatter technology, or actively transmit data based on RA technique. Moreover, to deal with the dynamic and uncertainty of jamming attacks, we develop a new Markov decision process framework with two decision epochs over one time slot to formulate the anti-jamming deception strategy for the transmitter and then use the Q-learning algorithm to maximize the long-term average throughput for the legitimate communication system. Although the Q-learning algorithm is an effective tool to help the transmitter obtain the optimal policy without requiring jammer’s information in advance, its convergence is usually very slow and might not be efficient to implement in practice. Thus, we develop a novel deep dueling reinforcement learning algorithm that enables the transmitter to obtain the optimal policy thousand times faster than those of the conventional reinforcement learning methods, e.g., Q-learning and deep Q-learning algorithms. The key idea of this algorithm is dividing the deep neural network into two sequences, i.e.,

streams, of fully connected layers to separately estimate the values of states and advantages of actions, and thus the convergence rate can be significantly improved. It is worth noting that the reactive jammer can adjust its attack policy by sensing the activities of the transmitter on the channel, e.g., actively transmit or idle. Thus, with a very fast convergence rate, our proposed solution can quickly and efficiently adapt the optimal defense strategy when the jammer adjusts its policy. Extensive simulation results then show that our proposed solution can achieve a very good performance in terms of throughput and packet loss compared with other conventional anti-jamming strategies. Interestingly, we show that with our proposed solution, the transmitter can utilize the power from jamming signals, and thus the more power the jammer uses to attack the channel, the greater performance we can achieve.

The key contributions of the paper are summarized as follows:

- Propose the intelligent anti-jamming deception strategy that can not only undermine the jammer's attack ability, but also leverage the jammer's power to enhance the system performance.
- Introduce the novel ideas of using RF energy harvesting and ambient backscatter techniques which can further exploit jamming signals to achieve greater performance.
- Develop a new MDP model to deal with reactive jamming attacks and propose the reinforcement algorithm to help the transmitter obtain the optimal defense policy without requiring information about jammer in advance.
- Propose the deep dueling algorithm with a novel neural network architecture to quickly obtain the optimal defense policy for the system.
- Perform extensive simulations to show the efficiency of our proposed solutions as well as to study key factors which have significant impacts in defeating reactive jamming attacks.

The rest of paper is organized as follows. Section II and Section III describe the system model and the problem formulation, respectively. Section IV presents the Q-learning and deep Q-learning algorithms. Then, the deep dueling algorithm is introduced in Section V. After that, the simulation results are discussed in Section VI. Finally, conclusions are drawn in Section VII.

## II. SYSTEM MODEL

We consider a wireless system in which a transmitter communicates with a receiver through a dedicated channel  $C$  as shown in Fig. 1. In particular, the transmitter is equipped with a data queue to store data before transmitting to the receiver. The maximum data queue size is denoted by  $D$ . When a new packet arrives at the transmitter, if the data queue is not full, the packet will be stored in the queue. Otherwise, the packet will be dropped. We assume that time is

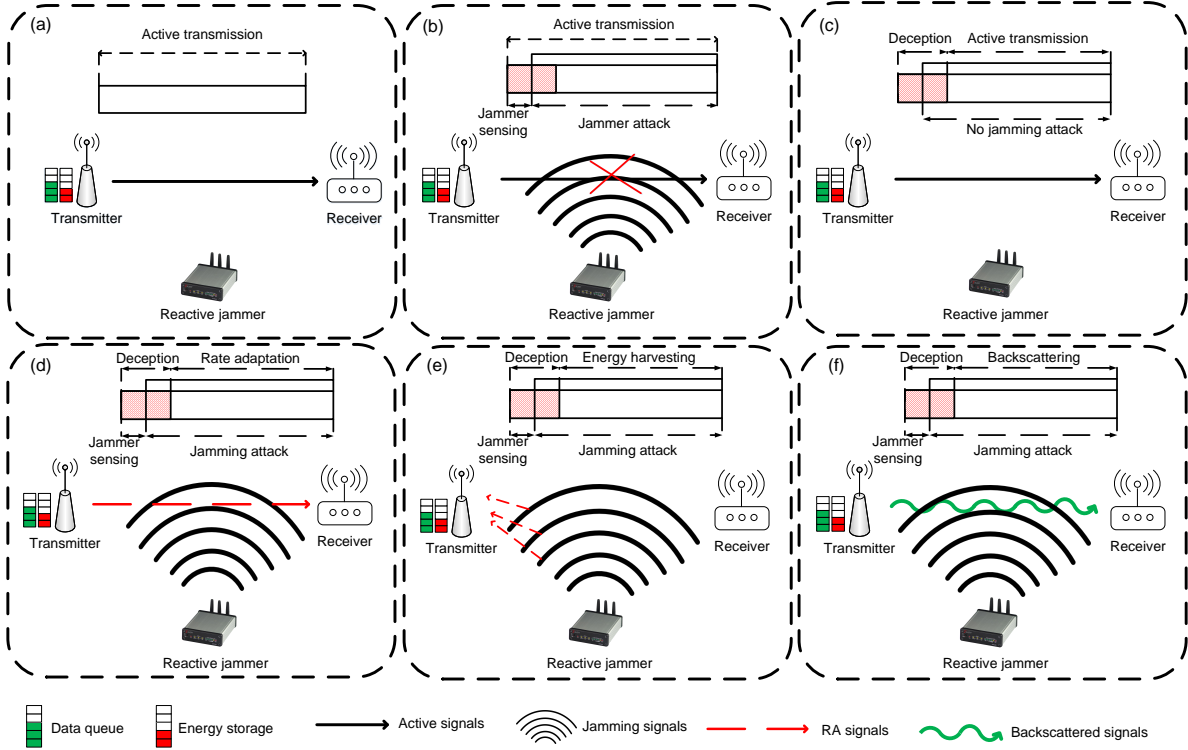


Fig. 1: An illustration of deception strategy to deal with reactive jamming attacks.

slotted, and at each time slot there are  $K$  packets arriving at the data queue with probability  $\lambda$ . Additionally, the transmitter is equipped with an energy harvesting circuit and an energy storage. By using the energy harvesting technology, the transmitter can harvest energy from the jamming signals when the jammer attacks the channel. The harvested energy will then be stored in the energy storage to support operations of the transmitter. The maximum energy storage capacity is denoted by  $E$ . In addition to harvest energy from jamming signals, the transmitter is also able to harvest energy from surrounding RF signals, and we assume that the transmitter can harvest  $e_v$  units of energy with probability  $p_e$  at each time slot. For example, a fundamental energy unit can be considered to be  $60 \mu J$  [32]. The transmitter is also equipped with an ambient backscatter circuit [18] to be able to backscatter data to its receiver if the jammer attacks the channel.

#### A. Reactive Jammer

In this work, we consider a powerful reactive jammer<sup>1</sup> which can attack the channel when it detects active transmissions from the transmitter. Intuitively, based on a common signal detection

<sup>1</sup>Note that our system model can be extended straightforwardly to the case with multiple jammers which can cooperatively attack the channel, i.e., only one jammer attacks the channel at a time.

mechanism, e.g., energy detection [23], [24], the jammer can detect the activity of the transmitter and attack the channel by transmitting strong signals to the channel to reduce the effective signal-to-interference-plus-noise ratio (SINR) at the receiver. In particular, under the jammer attack, the SINR at the receiver can be formally expressed by [1], [12]:

$$\theta = \frac{P^R}{\phi P^J + \rho^2}, \quad (1)$$

where  $P^R$  is the received power from the transmitter at the receiver,  $\phi P^J$  expresses the jamming power received at the receiver in which  $0 \leq \phi \leq 1$  is an attenuation factor, and  $\rho^2$  is the variance of additive white Gaussian noise. We denote  $P_{\text{avg}}$  as the time-average power constraint of the jammer and  $P_{\text{max}}$  as the peak jamming power, i.e.,  $P_{\text{avg}} \leq P_{\text{max}}$  [12].

In this work, once detecting activities of the transmitter on the target channel, the reactive jammer can attack the channel with different power levels at different probabilities. This strategy is much more intelligent and beneficial for the jammer than the fixed strategy, i.e., always attack at the same power level, as the jammer can adjust its attack power levels based on the activities of the transmitter, e.g., actively transmit, use the RA technique or stay idle. Let  $\mathbf{P}_J = \{P_0^J, \dots, P_n^J, \dots, P_N^J\}$  denote the vector of  $N$  discrete jamming power levels. We denote  $\mathbf{x} \triangleq (x_0, \dots, x_n, \dots, x_N)$  as an attack probability vector. In each time slot, if the transmitter actively transmits data on the target channel, the jammer can select any transmit power level  $P_n^J$  as long as its average power constraint is satisfied. Then, the attack strategy space of the jammer  $\mathbf{J}_s$  can be defined as follows:

$$\mathbf{J}_s \triangleq \left\{ (x_0, \dots, x_n, \dots, x_N), \sum_{n=0}^N x_n = 1, x_n \in [0, 1], \forall n \in \{0, \dots, N\}, \mathbf{x} \mathbf{P}_J^\top \leq P_{\text{avg}} \right\}. \quad (2)$$

### B. Deception Strategy

In this paper, we propose an intelligent deception mechanism that allows the system to not only undermine the jammer's attack efficiency but also leverage the jamming signals to improve the system performance. In particular, at the beginning of each time slot, the transmitter can lure the jammer by actively transmitting signals for a short period of time<sup>2</sup>. In this case, if the jammer attacks the channel, the transmitter can leverage the jamming signals to support its operations. This strategy is very beneficial for low-power systems even in dealing with a very powerful reactive jammer. The reason is that if the jammer often attacks the channel at high

<sup>2</sup>It is noted that the deception time must be higher than the detection time of the jammer. The transmitter can observe the activities of jammer during the learning process, and then determine the optimal deception time. Determining the optimal deception time is out of scope of this paper.

power levels, the jammer will unintentionally provide an abundant energy resource to supply for the legitimate system.

In the system under considerations, we assume that time is slotted, and at the beginning of a time slot, the transmitter can choose to actively transmit data or perform deception strategy. If the transmitter chooses to actively transmit data and the jammer does not attack the channel (as illustrated in Fig. 1(a)), the transmitter can successfully transmit maximum  $\hat{d}_a$  packets. If the jammer attacks the channel, the transmitter cannot actively transmit packets to the receiver as shown in Fig. 1(b). Each packet requires  $e_r$  units of energy to be successfully transmitted. On the other hand, if the transmitter performs the deception, it will first transmit signals on the channel for a short period. After that, the transmitter listens the channel to detect activities of the jammer. We denote  $e_f$  as the total amount of energy that the transmitter needs to perform deception (including the sensing process). If the jammer does not attack the channel after deception, the transmitter can choose to actively transmit maximum  $\hat{d}_{de}$  packets to the receiver in the rest of the time slot ( $\hat{d}_{de} < \hat{d}_a$ ) as illustrated in Fig. 1(c). In contrast, if the jammer attacks the channel, the transmitter can choose one of three actions: (i) reduce transmission rate by using the RA technique, (ii) harvest energy from the jamming signals, or (iii) backscatter data through the jamming signals as illustrated in Fig. 1(d), Fig. 1(e), and Fig. 1(f) respectively.

1) *Rate Adaptation*: Based on jamming power  $P_n^J$ , the transmitter can actively transmit data at maximum rate  $r_m$  by using the rate adaptation technique. We then denote  $\mathbf{r} = \{r_1, \dots, r_m, \dots, r_M\}$  as the set of  $M$  transmission rates that the transmitter can support to transmit data under jamming attacks. At each rate  $r_m$ , the transmitter can transmit maximum  $\hat{d}_m^r$  packets. We define  $\gamma_m$  as the lowest SINR value at which the receiver can successfully decode packets sent at rate  $r_m$ . The higher transmission rate requires the higher value of SINR at the receiver [1]. Thus, for  $m = 1, \dots, M$ , when  $\gamma_{m-1} \leq \theta < \gamma_m$ , the receiver only can decode packets sent at rates  $r_0, r_1, \dots, r_{m-1}$ , and the packets sent at rate  $r_m$  or higher will be completely lost [1]. To detect the states of the jammer, i.e., idle or attack, after deception, several detection techniques can be adopted, e.g., energy detection [23], [24]. If the transmitter fails to detect the attack power level of the jammer, the transmitted packets will be lost. We then denote  $p_{\text{miss}}$  as the miss detection probability of the transmitter in detecting attack power levels of the jammer.

2) *RF Energy Harvesting*: If the jammer attacks the channel with power level  $P_n^J$  (after the transmitter performs the deception), the transmitter can harvest  $e_n^J$  units of energy from the jamming signals through the energy harvesting circuit and then store the harvested energy in the energy storage to support for future deception and actual transmission activities [18]. We then denote  $\mathbf{e} = \{e_0^J, \dots, e_n^J, \dots, e_N^J\}$  as the amount of energy that the transmitter can successfully

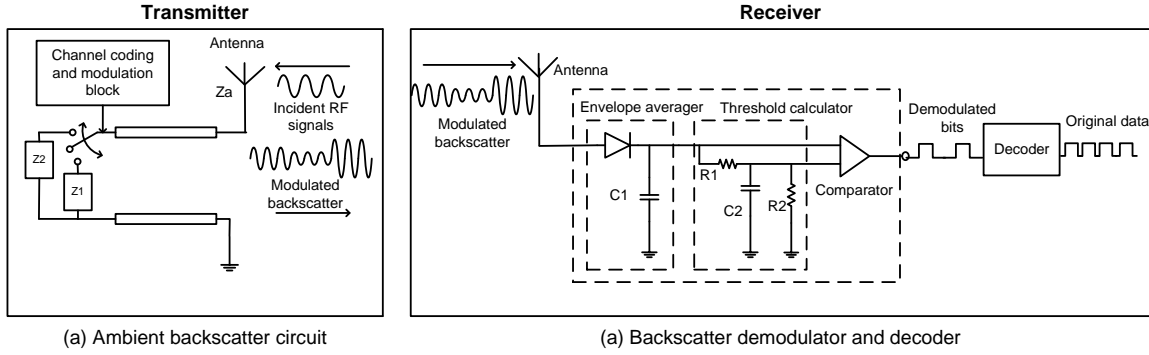


Fig. 2: Ambient backscatter circuit.

harvest from the jamming signals according to the attack power levels of the jammer. Intuitively, the more power the jammer uses to attack the channel, the more energy the transmitter can successfully harvest from the jamming signals. This proportional relationship can be observed clearly through the Friis equation [19] in which the amount of harvested energy can be expressed by a linear function of transmission power of the jammer.

3) *Ambient Backscatter Communications*: The transmitter can also backscatter the jamming signals to transmit data to the receiver by using the ambient backscatter circuit as shown in Fig. 2(a) [20]. In particular, by switching between two loads  $Z_1$  and  $Z_2$  with an RF switch, e.g., ADG902, the transmitter can switch between two states: (i) reflecting and (ii) non-reflecting. At the non-reflecting state, all the RF signals (i.e., the jamming signals in this paper) will be absorbed, and thus this state represents bits ‘0’. Otherwise, at the reflecting state, all the RF signals will be reflected to the receiver, and thus this state represents bits ‘1’. As such, with ambient backscatter technology, the transmitter can backscatter data to the receiver without requiring any active component. It is worth noting that at the non-reflecting state, the transmitter can harvest energy from the RF signals, but the amount of the harvested energy is relatively small and only suitable for operations of the backscatter mode. Through many real experiments and analysis on backscatter communication systems in the literature, e.g., [20], [21], [22], it can be observed that the more power the RF source uses to transmit signals (i.e., the jammer attacks the channel at high power levels), the more energy per information bit the transmitter can backscatter to the receiver, and thus the less Bit Error Rate (BER) of backscatter communication is. This also implies that the more packets the transmitter can successfully transmit to the receiver by backscattering the jamming signals when the jammer uses higher power levels to attack. It is worth noting that several ambient backscatter prototypes have been introduced in the literature with backscatter rates up to few Mbps [18]. Thus, using ambient backscatter to leverage the

strong jamming signals is a very promising solution.

If the jammer attacks the channel with power level  $P_n^J$  after deception, the transmitter can transmit maximum  $\hat{d}_n^J$  packets to the receiver through using the backscatter technique. We denote  $\hat{\mathbf{d}} = \{\hat{d}_0^J, \dots, \hat{d}_n^J, \dots, \hat{d}_N^J\}$  as the number of packets that the transmitter can successfully backscatter to the receiver when the jammer attacks the channel with power level  $\mathbf{P}_J = \{P_0^J, \dots, P_n^J, \dots, P_N^J\}$ , respectively. Note that the backscatter rate depends on the hardware configuration, i.e., the values of the RC circuit elements in Fig. 2(b) [20]. Thus, in this work, we consider that the backscatter rate is fixed at a maximum rate of  $d_{\max}$  packets. If the maximum number of packets that can be backscattered at jamming power  $P_n^J$  is lower than  $d_{\max}$ ,  $(d_{\max} - \hat{d}_n^J)$  packets will be lost as the jamming signals is not strong enough to support the transmitter to transmit all  $d_{\max}$  packets.

To decode the backscattered signals, there are two approaches: (i) using an analog-to-digital converter (ADC) and (ii) using the averaging mechanism [20], [18]. However, as the ADC consumes a significant amount of energy, the averaging mechanism is usually adopted in the literature (especially in IoT networks) to allow the receiver to decode the backscattered signals by using analog components as illustrated in Fig. 2(b). The key idea of the averaging mechanism is using the envelope-averaging circuit to smooth the backscattered signals received at the receiver. Then, the voltage between low and high levels of the smoothed signals is calculated by the compute-threshold circuit. Finally, the comparator compares this voltage with a predefined threshold to derive output bits, i.e., zero and one, properly. More information about decoding algorithms and hardware designs can be found in [20].

### C. Jammer Performance Analysis

To theoretically elaborate the efficiency of proposed deception mechanism, in the following, we evaluate the jammer utility under the transmitter's deception strategy. At the beginning of each time slot, if the transmitter actively transmits actual data, and if the jammer attacks the channel, all packets transmitted by the transmitter are lost. In this case, the jammer can receive a reward of  $0 \leq d_a \leq \hat{d}_a$  (corresponding to the number of dropped packets). Thus, the jammer's utility function for this case can be expressed as follows:

$$U_1^J = \begin{cases} d_a & \text{if the transmitter transmits actual data and the jammer attacks the channel.} \\ -d_a & \text{if the transmitter transmits actual data and the jammer does not attack the channel.} \end{cases} \quad (3)$$

If the transmitter chooses to use  $e_f$  units of energy to perform the deception, the jammer will get a reward of  $\frac{e_f}{e_r}$ . Here,  $\frac{e_f}{e_r}$  can be interpreted as the potential number of packets that the transmitter can transmit without performing deception. If the jammer decides to attack the

channels, the transmitter can leverage the jamming signals to harvest  $e_n^J$  units of energy or backscatter  $0 \leq d_n^J \leq \hat{d}_n^J$  packets or using the rate adaptation to transmit  $0 \leq d_m^r \leq \hat{d}_m^r$  packets. Note that the harvested energy can be used to actively transmit data or perform deception actions later. Thus, the penalty for the jammer if the transmitter harvests energy from the jamming signals can be expressed by  $-\frac{e_n^J}{e_r}$ , i.e., the number of potential packets which the transmitter can transmit from the harvested energy. Similarly, we can denote  $-d_n^J$  and  $-d_m^r$  to be the penalties for the jammer if the transmitter uses backscatter and rate adaptation techniques to transmit data, respectively. Hence, the utility function of the jammer in this case can be expressed as follows:

$$U_2^J = \begin{cases} \frac{e_f}{e_r} - \frac{e_n^J}{e_r} & \text{if the transmitter harvests energy from the jamming signals,} \\ \frac{e_f}{e_r} - d_n^J & \text{if the transmitter backscatters data through the jamming signals,} \\ \frac{e_f}{e_r} - d_m^r & \text{if the transmitter adapts its transmission rate,} \\ \frac{e_f}{e_r} & \text{if the transmitter stays idle.} \end{cases} \quad (4)$$

Finally, if the transmitter performs deception, but the jammer does not attack the channel, then the transmitter can actively transmit data in the rest of the time slot. In this case, the transmitter will waste  $e_f$  units of energy for the deception action, but it can successfully transmit  $0 \leq d_{de} \leq \hat{d}_{de}$  packets to the receiver. Thus, we can derive the utility function of the jammer in this case as follows:

$$U_3^J = \begin{cases} \frac{e_f}{e_r} - d_{de} & \text{if the transmitter transmits data,} \\ \frac{e_f}{e_r} & \text{if the transmitter stays idle.} \end{cases} \quad (5)$$

Then, we derive the jammer's expected overall utility as follows:

$$U = U_1^J + U_2^J + U_3^J. \quad (6)$$

In (6), it can be observed that if the jammer attacks the channel at high frequency and at the same time the transmitter often performs deception strategy, then the efficiency of jamming attack will be significantly reduced. However, if the jammer does not often attack the channel and the deception probability is high, then the deception strategy is not effective. As a result, in order to maximize the performance for the system, the transmitter needs to know the jammer's strategy, e.g., power levels and frequency of attacks, in advance. Unfortunately, this information is usually unknown by the transmitter in advance. Thus, in this paper, we propose reinforcement learning approaches to enable the transmitter to deal with the uncertainty and dynamic of the jammer and the environment by learning from real-time interactions.

Note that the amount of harvested energy and the number of backscattered/transmitted packets, i.e.,  $d_a$ ,  $d_{de}$ ,  $d_n^J$ ,  $e_n^J$ , and  $d_m^r$ , can be observed after interacting with the jammer. Thus, our proposed solutions do not require this explicit information in advance. Instead, the learning algorithms

learn these values and find the optimal policy for the transmitter. For example, in the case if the jammer often attacks the channel at low power levels, the number of backscattered packets and the amount of harvested energy could be low. As such, our proposed reinforcement learning algorithms can learn and find the optimal policy to guide the transmitter to choose the best actions, e.g., rate adaptation instead of backscattering, to maximize the system performance.

### III. PROBLEM FORMULATION

To learn from and adapt with the jammer's behaviors as well as the uncertainty of the environment, we adopt the Markov decision process (MDP) framework to formulate the optimization problem. The MDP is defined by a tuple  $\langle \mathcal{S}, \mathcal{A}, r \rangle$  where  $\mathcal{S}$  is the state space,  $\mathcal{A}$  is the action space, and  $r$  is the immediate reward function of the system. For a conventional MDP process, at the beginning of a time slot, the transmitter observes the current system state, e.g., data, energy and channel states, performs an action, e.g., active data transmission or deception, and observes the results in the end of the time slot, e.g., packets are successfully transmitted or dropped. However, this conventional process is not appropriate to adopt in our model to defeat the reactive jammer. The reason is that the reactive jammer only attacks channel if it detects activities of the transmitter on the channel, and thus at the beginning of a time slot, the channel state is always idle. Second, for the conventional MDP process with only one decision epoch, after the transmitter performs deception and the jammer attacks the channel, we only can undermine the jammer's power, but cannot leverage jamming signals for enhancing the system performance. We thus propose a new MDP model with two decision epochs, i.e., one at the beginning of a time slot and another is after the deception period as illustrated in Fig. 3. To be more specific, at the first decision epoch, i.e., at the beginning of a time slot, the transmitter observes the current system state, including data queue, energy queue, deception and channel states, and makes an action, e.g., deception or actively transmit actual data. Then, at the beginning of the second decision epoch, i.e., right after the deception period, the transmitter observes the new states, e.g., whether the jammer attacks the channel or not, and then makes an action, e.g., backscatter or harvest energy from jamming signals if the jammer attacks the channel. In this way, we can not only undermine the jammer's power, but also utilize its power for improving the system performance.

#### A. State Space

The state space of the system can be defined as follows:

$$\mathcal{S} \triangleq \left\{ (f, j, d, e) \mid f \in \{0, 1\}; j \in \{0, 1\}; d \in \{0, \dots, D\}; e \in \{0, \dots, E\} \right\} \setminus \{0, 1, d, e\}, \quad (7)$$

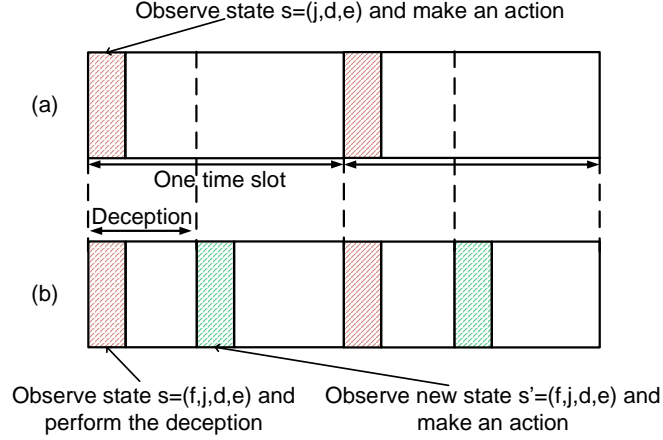


Fig. 3: Decision epoch of (a) conventional MDP and (b) proposed MDP.

where  $d$  and  $e$  represent the number of packets in the data queue and the number of energy units in the energy storage of the transmitter, respectively.  $D$  and  $E$  are the maximum data queue size and energy storage capacity, respectively.  $f$  represents the deception strategy of transmitter, i.e.,  $f = 1$  when the deception is performed and  $f = 0$  otherwise. Note that  $f$  is always 0 at the first epoch, but could be 0 or 1 in the second epoch of a time slot.  $j$  represents the state of the jammer, i.e.,  $j = 1$  when the jammer attacks the channel and  $j = 0$  otherwise. Note that at the first epoch of a time slot,  $j$  is always 0. However, after the deception is made,  $j$  could be 0 or 1. Moreover, at the second epoch, the jammer only attacks the channel if the transmitter performs the deception at the first epoch. Thus, the system state space does not include state  $s = \{0, 1, d, e\}$ . The system state is then defined as a composite variable  $s = (f, j, d, e) \in \mathcal{S}$ .

### B. Action Space

We denote  $\mathcal{A} \triangleq \{a : a \in \{0, 1, \dots, 4 + m\}\}$  as the action space of the transmitter in which  $a = 1$  represents the action of performing the deception. At the beginning of a time slot, if the transmitter has enough energy (i.e.,  $e \geq e_f$ ), it can choose to perform the deception. In this case, we have the following actions:

$$a = \begin{cases} 2, & \text{the transmitter transmits data if } f = 1, j = 0, d > 0, \text{ and } e > e_r, \\ 3, & \text{the transmitter harvests energy if } f = 1, j = 1, \text{ and } e < E, \\ 4, & \text{the transmitter backscatters data if } f = 1, j = 1, \text{ and } d > 0, \\ 4 + m, & \text{the transmitter adapts its transmission to rate } r_m \text{ if } f = 1, j = 1, d > 0, \text{ and } e > e_r, \\ 0, & \text{the transmitter stays idle.} \end{cases} \quad (8)$$

In particular, after performing the deception, the transmitter listens to the channel. If the jammer does not attack the channel, i.e.,  $j = 0$ , the data queue is not empty, and there is enough energy in the energy storage, the transmitter can choose to actively transmit data to the receiver in the rest of the time slot. If the jammer attacks the channels, i.e.,  $j = 1$ , the transmitter can choose to harvest energy from the jamming signals in the rest of the time slot. If the data queue is not empty, the transmitter can choose to backscatter data to the receiver in the rest of the time slot. Additionally, the transmitter can choose to reduce its data rate to actively transmit data to the receiver if it has data in the data queue and has enough energy for active transmissions in the energy storage. Otherwise, the transmitter can choose to stay idle for the rest of the time slot.

If the transmitter decides not to perform the deception at the beginning of the time slot, we have the following actions:

$$a = \begin{cases} 2, & \text{the transmitter actively transmits data if } d > 0 \text{ and } e > e_r, \\ 0, & \text{the transmitter stays idle.} \end{cases} \quad (9)$$

Specifically, in this case, the transmitter can choose to actively transmit data if it has data in the data queue and has enough energy in the energy storage for active transmissions. Alternatively, the transmitter can decide to stay idle in this time slot. The flowchart of the transmitter's actions is illustrated in Fig. 4.

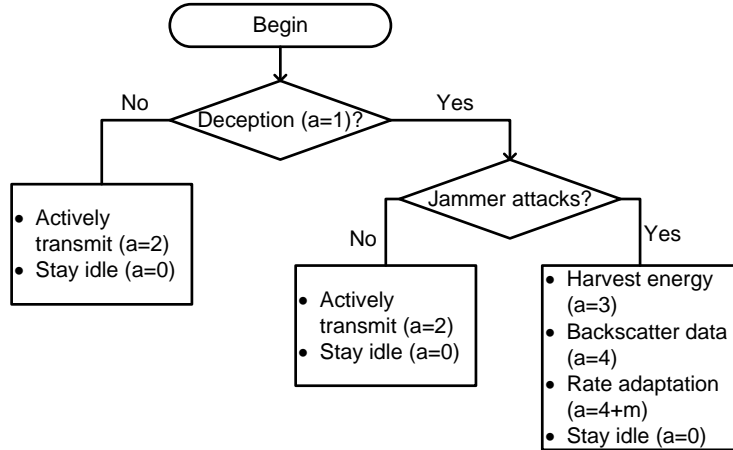


Fig. 4: Flowchart to express actions of transmitter.

### C. Immediate Reward

We define the reward function for the system as the number of packets that are successfully transmitted to the receiver. Thus, the immediate reward of the system over one time slot after

the transmitter takes an action  $a$  at state  $s$  can be defined as follows:

$$r(s, a) = \begin{cases} d_a, & \text{if } a = 2 \text{ and } f = 0, \\ d_{de} & \text{if } a = 2 \text{ and } f = 1, \\ d_n^J, & \text{if } a = 4, \\ d_m^r, & \text{if } a = 4 + m, \\ 0, & \text{otherwise.} \end{cases} \quad (10)$$

In (10), if the transmitter chooses to actively transmit data at the beginning of a time slot and the jammer does not attack the channel, it can successfully transmit  $d_a \leq \hat{d}_a$  packets to the receiver. If the transmitter performs deception and the jammer does not attack the channel, the transmitter can transmit  $d_{de} \leq \hat{d}_{de}$  packets to the receiver. However, if the transmitter performs deception and the jammer attacks the channel, the transmitter can backscatter  $d_n^J \leq \hat{d}_n^J$  packets or transmit  $d_m^r \leq \hat{d}_m^r$  packets (using rate adaption technique) to the receiver. Note that the rewards of harvesting energy from jamming signals and deception activities can be captured by the number of packets which are successfully transmitted to the receiver. Finally, the immediate reward is 0 if the transmitter cannot successfully transmit any packet to the receiver.

Note that after performing an action, the transmitter observes its reward, i.e., the number of packets that are successfully transmitted based on ACK messages sent from the receiver. In other words,  $d_a$ ,  $d_{de}$ ,  $d_n^J$ , and  $d_m^r$  are the actual number of packets received at the receiver. As such, the reward function captures the overall path between the receiver and the transmitter, e.g., end-to-end SNR, BER, or fading.

#### D. Optimization Formulation

In this work, we aim to obtain the optimal defense policy to maximize the average long-term throughput of the system, denoted by  $\pi^* : \mathcal{S} \rightarrow \mathcal{A}$ . In particular, the optimal policy is a mapping from a given state, i.e., data queue, energy level, jammer state, and deception status, to an optimal action. The optimization problem is then expressed as follows:

$$\max_{\pi} \quad \mathcal{R}(\pi) = \lim_{T \rightarrow \infty} \frac{1}{T} \sum_{k=1}^T \mathbb{E}(r_k(s_k, \pi(s_k))), \quad (11)$$

where  $r_k(s_k, \pi(s_k))$  is the immediate reward under policy  $\pi$  at time step  $k$  and  $\mathcal{R}(\pi)$  is the average reward of the transmitter under the policy  $\pi$ . In Theorem 1, we show that the average throughput  $\mathcal{R}(\pi)$  is well defined and does not depend on the initial state.

**THEOREM 1.** *For every  $\pi$ , the average throughput  $\mathcal{R}(\pi)$  is well defined and does not depend on the initial state.*

The proof of Theorem 1 is provided in Appendix A.

## IV. OPTIMAL DEFENSE STRATEGY WITH REINFORCEMENT LEARNING ALGORITHMS

### A. *Q-Learning based Deception Strategy*

In this section, we propose the Q-learning algorithm to deal with the dynamic and uncertainty of the jammer. In particular, this algorithm does not require the information about the jammer in advance. Instead, it learns from the previous experiences to find the optimal defense policy for the transmitter. According to [26], it was proved that the Q-learning algorithm will converge to the optimal policy with probability one after a finite number of iterations. In the following, we present the key idea behind the Q-learning algorithm.

We denote  $\pi^* : \mathcal{S} \rightarrow \mathcal{A}$  as the optimal defense policy, which is a mapping from system states to their corresponding actions, for the transmitter under the jamming attacks. For each policy  $\pi$ , the expected value function  $\mathcal{V}^\pi(s) : \mathcal{S} \rightarrow \mathbb{R}$  can be expressed as follows:

$$\mathcal{V}^\pi(s) = \mathbb{E}_\pi \left[ \sum_{t=0}^{\infty} \gamma r_t(s_t, a_t) | s_0 = s \right] = \mathbb{E}_\pi \left[ r_t(s_t, a_t) + \gamma \mathcal{V}^\pi(s_{t+1}) | s_0 = s \right], \quad (12)$$

where  $r_t(s_t, a_t)$  is the immediate reward achieved after performing action  $a_t$  at state  $s_t$  and  $0 \leq \gamma < 1$  is the discount factor which represents the importance of long-term reward [26]. To find the optimal policy  $\pi^*$ , the optimal action at each state can be found by using the following optimal value function.

$$\mathcal{V}^*(s) = \max_a \left\{ \mathbb{E}_\pi [r_t(s_t, a_t) + \gamma \mathcal{V}^\pi(s_{t+1})] \right\}, \quad \forall s \in \mathcal{S}. \quad (13)$$

Thus, the optimal Q-functions for all pairs of states and actions are derived as follows:

$$\mathcal{Q}^*(s, a) \triangleq r_t(s_t, a_t) + \gamma \mathbb{E}_\pi [\mathcal{V}^\pi(s_{t+1})], \quad \forall s \in \mathcal{S}. \quad (14)$$

Then, the optimal value function  $\mathcal{V}^*(s)$  can be written as  $\mathcal{V}^*(s) = \max_a \{\mathcal{Q}^*(s, a)\}$ . By making samples iteratively, the problem is reduced to determining the optimal value of Q-function, i.e.,  $\mathcal{Q}^*(s, a)$ , for all state-action pairs. In particular, the Q-function is updated according to (15).

$$\mathcal{Q}_{t+1}(s_t, a_t) = \mathcal{Q}_t(s_t, a_t) + \tau_t \left[ r_t(s_t, a_t) + \gamma \max_{a_{t+1}} \mathcal{Q}_t(s_{t+1}, a_{t+1}) - \mathcal{Q}_t(s_t, a_t) \right]. \quad (15)$$

Specifically, (15) is used to find the temporal difference between the predicted Q-value, i.e.,  $r_t(s_t, a_t) + \gamma \max_{a_{t+1}} \mathcal{Q}_t(s_{t+1}, a_{t+1})$  and its current value, i.e.,  $\mathcal{Q}_t(s_t, a_t)$ . The learning rate  $\tau_t$  determines the impact of new information to the existing value. During the learning process, the learning rate can be adjusted dynamically, or it can be chosen to be a constant. To guarantee the convergence for the Q-learning algorithm, the learning rate  $\tau_t$  is deterministic, nonnegative, and satisfies the following conditions [26]:

$$\tau_t \in [0, 1], \sum_{t=1}^{\infty} \tau_t = \infty, \text{ and } \sum_{t=1}^{\infty} (\tau_t)^2 < \infty. \quad (16)$$

Based on (15), the algorithm updates the Q-values for all state-action pairs. In particular, based on the  $\epsilon$ -greedy algorithm, at the current state  $s_t$ , the algorithm selects a random action with probability  $\epsilon$  and selects an action that maximizes the Q-value function with probability  $1 - \epsilon$ . After performing the chosen action, the algorithm observes the next system state and immediate reward to update the Q-table based on (15). After a finite number of iterations, the algorithm will obtain the optimal defense policy for the system [26]. Nevertheless, the Q-learning based algorithms are well-known for their slow-convergence, especially in complicated systems with high-dimensional state and actions spaces. To deal with this problem, in the following, we propose the deep dueling algorithm to allow the transmitter to obtain the optimal policy with a much faster convergence rate by leveraging the deep Q-learning and novel dueling architecture.

### B. Deep Q-Learning based Deception Strategy

In this section, we propose the deep Q-learning algorithm [27] to cope with the slow-convergence problem of the Q-learning algorithm introduced in Section IV. The deep Q-learning algorithm implements a deep neural network instead of the Q-table to find the approximated values of  $\mathcal{Q}^*(s, a)$ .

According to [27], the performance of reinforcement learning approaches might not be stable or even diverges when using a nonlinear function approximator. The reason is that with a small change of Q-values, the data distribution and correlations between the Q-values and the target values, i.e.,  $r + \gamma \max_a \mathcal{Q}(s, a)$ , are varied, and thus the policy is greatly affected. To address this issue, we use three mechanisms, i.e., experience replay, target Q-network, and feature set.

- *Experience replay mechanism:* The algorithm implements a replay memory  $\mathbf{D}$ , i.e., memory pool, to store transitions  $(s_t, a_t, r_t, s_{t+1})$  instead of running on state-action pairs as they occur during experience. Random samples from the memory pool are then fed to the deep neural network for training. In this way, the algorithm can efficiently learn from previous experiences many times and remove the correlations between observations [27].
- *Quasi-static target Q-network:* Obviously, the Q-values will be changed during the training process. As a result, the value estimations can be out of control if a constantly shifting set of values is used to update the Q-network resulting in the destabilization of the algorithm. To overcome this issue, the deep Q-learning algorithm implements a target Q-network to frequently but slowly update to the primary Q-network. As such, the correlations between the target and estimated Q-values are significantly eliminated, thereby stabilizing the algorithm.
- *Feature set:* For each state, we determine four features including the activities of the jammer and the status of the deception as well as the status of data and energy queues

of the transmitter. These features are then fed to the deep neural network to approximate Q-values for each state-action pair. Doing so, all aspects of each state are trained resulting in a high convergence rate.

---

**Algorithm 1** Deep Q-learning Based Anti-jamming Algorithm

---

- 1: Initialize replay memory  $\mathbf{D}$  to capacity  $\mathcal{D}$ .
- 2: Initialize the Q-network  $\mathcal{Q}$  with random weights  $\theta$ .
- 3: Initialize the target Q-network  $\hat{\mathcal{Q}}$  with weight  $\theta^- = \theta$ .
- 4: **for**  $episode=1$  to  $I$  **do**
- 5:     With probability  $\epsilon$  select a random action  $a_t$ , otherwise select  $a_t = \text{argmax } \mathcal{Q}^*(s_t, a_t; \theta)$ .
- 6:     Perform action  $a_t$  and observe reward  $r_t$  and next state  $s_{t+1}$ .
- 7:     Store transition  $(s_t, a_t, r_t, s_{t+1})$  in the replay memory  $\mathbf{D}$ .
- 8:     Sample random mini-batch of transitions  $(s_j, a_j, r_j, s_{j+1})$  from  $\mathbf{D}$ .
- 9:      $y_j = r_j + \gamma \max_{a_{j+1}} \hat{\mathcal{Q}}(s_{j+1}, a_{j+1}; \theta^-)$ .
- 10:     Perform a gradient descent step on  $(y_j - \mathcal{Q}(s_j, a_j; \theta))^2$  with respect to the network parameter  $\theta$ .
- 11:     Every  $C$  steps reset  $\hat{\mathcal{Q}} = \mathcal{Q}$ .
- 12: **end for**

---

Algorithm 1 provides the details of the deep Q-learning algorithm. In particular, the training phase consists of multiple episodes. At each episode, given the current state, the algorithm chooses an action based on the epsilon greedy algorithm. The algorithm will start with a fairly randomized policy and later slowly move to a deterministic policy. In other words, at the first episode,  $\epsilon$  is set at a large value, e.g., 0.9, and gradually decayed to a small value, e.g., 0.1. After that, the algorithm performs the selected action and observes results from taking this action, i.e., next state and reward. This transition is then stored in the replay memory for training process at later episodes. In the learning process, random samples of transitions from the replay memory will be fed into the neural network. The algorithm then updates the neural network by minimizing the following lost function.

$$L_i(\theta_i) = \mathbb{E}_{(s, a, r, s') \sim U(\mathbf{D})} \left[ \left( r + \gamma \max_{a'} \hat{\mathcal{Q}}(s', a'; \theta_i^-) - \mathcal{Q}(s, a; \theta_i) \right)^2 \right], \quad (17)$$

where  $\gamma$  is the discount factor,  $\theta_i$  are the parameters of the Q-networks at episode  $i$  and  $\theta_i^-$  are the parameters of the target network, i.e.,  $\hat{\mathcal{Q}}$ . Differentiating the loss function in (17) with respect to the parameters of the neural networks, we have the following gradient:

$$\nabla_{\theta_i} L(\theta_i) = \mathbb{E}_{(s, a, r, s')} \left[ \left( r + \gamma \max_{a'} \hat{\mathcal{Q}}(s', a'; \theta_i^-) - \mathcal{Q}(s, a; \theta_i) \nabla_{\theta_i} \mathcal{Q}(s, a; \theta_i) \right) \right]. \quad (18)$$

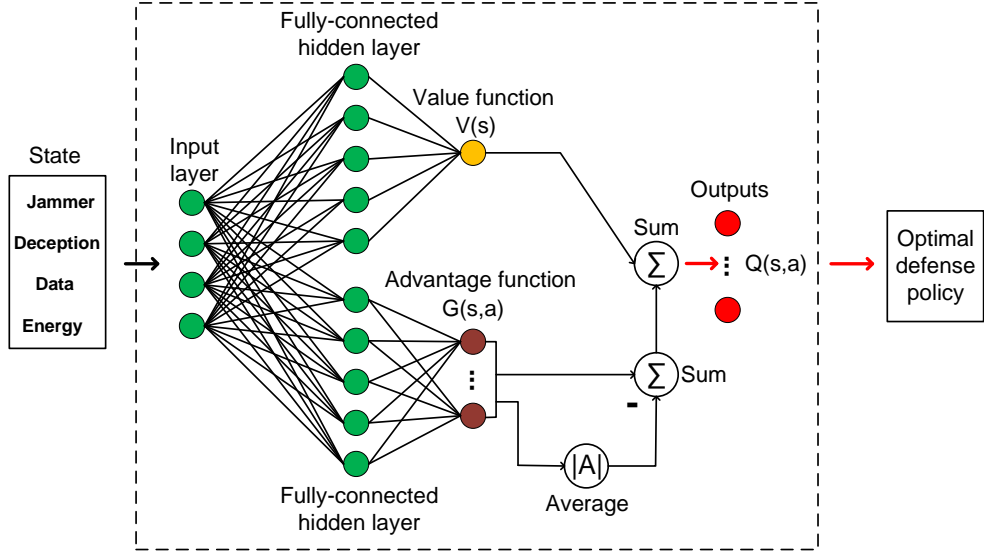


Fig. 5: Deep dueling neural network architecture based solution

The loss function is then minimized to update the parameters of the deep dueling network. After every  $C$  steps, the algorithm updates the target network parameters  $\theta_i^-$  with the Q-network parameters  $\theta_i$ . The target network parameters remain unchanged between individual updates.

## V. OPTIMAL DECEPTION STRATEGY WITH DEEP DUELING NEURAL NETWORK

### A. Deep Dueling Neural Network Architecture

According to [29], the convergence rate of the deep Q-learning algorithm is still limited due to the overestimation of the optimizer, especially in systems with large action and state spaces as considered in this work. Therefore, we propose a deep dueling algorithm [29], which was also originally developed by Google DeepMind in 2016, to further improve the system's convergence speed. The key idea making the deep dueling superior to conventional approaches is its novel neural network architecture. Clearly, in many states, it is unnecessary to estimate the value of corresponding actions as the choice of these actions has no repercussion on what happens [29]. For example, the rate adaptation actions only matter when the jammer attacks the channel at low power levels. Hence, instead of estimating the action-value function, i.e., Q-function, the algorithm divides the deep neural network into two sequences, i.e., streams, of fully connected layers to separately estimate the values of states and advantages of actions<sup>3</sup>. The

<sup>3</sup>The value function represents how good it is for the system to be in a given state. The advantage function is used to measure the importance of a certain action compared with others [29].

values and advantages are then combined at the output layer as shown in Fig. 5. In this way, the deep dueling algorithm can achieve more robust estimates of state value, and thus significantly improving its convergence rate as well as stability. Note that the flowchart of the deep dueling algorithm is the same as in the deep Q-learning. The main difference between the deep dueling algorithm and other conventional deep reinforcement learning algorithms is the deep dueling neural network. In the following, we present details of how to separate the Q-values into the value and the advantage functions.

Recall that given a stochastic policy  $\pi$ , the values of state-action pair  $(s, a)$  and state  $s$  are as follows:

$$\mathcal{Q}^\pi(s, a) = \mathbb{E}[r_t | s_t = s, a_t = a, \pi], \mathcal{V}^\pi(s) = \mathbb{E}_{a \sim \pi(s)}[\mathcal{Q}^\pi(s, a)]. \quad (19)$$

The advantage function of actions can be expressed as:

$$\mathcal{G}^\pi(s, a) = \mathcal{Q}^\pi(s, a) - \mathcal{V}^\pi(s). \quad (20)$$

Specifically, the value function  $\mathcal{V}$  corresponds to how *good it is to be in a particular state  $s$*  [29]. The state-action pair, i.e., Q-function, calculates the value of performing action  $a$  in state  $s$ . The advantage function decouples the state value from the Q-function to measure the importance of each action.

To estimate values of  $\mathcal{V}$  and  $\mathcal{G}$  functions, we use a dueling neural network in which one stream of fully-connected layers outputs a scalar  $\mathcal{V}(s; \beta)$  and the other stream estimates an  $|\mathcal{A}|$ -dimensional vector  $\mathcal{G}(s, a; \alpha)$ , where  $\alpha$  and  $\beta$  are the parameters of fully-connected layers. These two sequences are then combined at the output layer to obtain the Q-function by (21).

$$\mathcal{Q}(s, a; \alpha, \beta) = \mathcal{V}(s; \beta) + \mathcal{G}(s, a; \alpha). \quad (21)$$

Note that (21) applies to all  $(s, a)$  instances. Thus, to express (21) in a matrix form, one needs to replicate the scalar,  $\mathcal{V}(s; \beta)$ ,  $|\mathcal{A}|$  times. Importantly,  $\mathcal{Q}(s, a; \alpha, \beta)$  is a parameterized estimate of the true Q-function, and given  $\mathcal{Q}$ , we cannot obtain  $\mathcal{V}$  and  $\mathcal{G}$  uniquely. In other words, adding a constant to  $\mathcal{V}(s; \beta)$  and subtracting the same constant from  $\mathcal{G}(s, a; \alpha)$  result in the same Q-value. Therefore, (21) is unidentifiable resulting in a poor performance. To address this problem, the combining module of the network implements the following mapping:

$$\mathcal{Q}(s, a; \alpha, \beta) = \mathcal{V}(s; \beta) + (\mathcal{G}(s, a; \alpha) - \max_{a \in \mathcal{A}} \mathcal{G}(s, a; \alpha)). \quad (22)$$

In this way, the advantage function estimator has zero advantage when choosing action. Intuitively, given  $a^* = \operatorname{argmax}_{a \in \mathcal{A}} \mathcal{Q}(s, a; \alpha, \beta) = \operatorname{argmax}_{a \in \mathcal{A}} \mathcal{G}(s, a; \alpha)$ , we have  $\mathcal{Q}(s, a^*; \alpha, \beta) =$

$\mathcal{V}(s; \beta)$ . Therefore, we can convert (22) into a simple form by replacing the max operator with an average as follows:

$$\mathcal{Q}(s, a; \alpha, \beta) = \mathcal{V}(s; \beta) + \left( \mathcal{G}(s, a; \alpha) - \frac{1}{|\mathcal{A}|} \sum_a \mathcal{G}(s, a; \alpha) \right). \quad (23)$$

Note that subtracting the mean in (23) solves the unidentifiable problem. However, it does not change the relative rank of the advantage function values, and hence the Q-values for actions at each state. Based on (23) and the advantages of the deep reinforcement learning, we develop the

---

**Algorithm 2** Deep Dueling Neural Network Based Anti-jamming Algorithm

---

- 1: Initialize replay memory  $\mathbf{D}$  to capacity  $\mathcal{D}$ .
- 2: Initialize the primary network  $\mathcal{Q}$  including two fully-connected layers with random weights  $\alpha$  and  $\beta$ .
- 3: Initialize the target network  $\hat{\mathcal{Q}}$  as a copy of the primary Q-network with weights  $\alpha^- = \alpha$  and  $\beta^- = \beta$ .
- 4: **for**  $episode=1$  to  $I$  **do**
- 5:     Base on the  $\epsilon$ -greedy algorithm, with probability  $\epsilon$ , select a random action  $a_t$  at state  $s_t$ .  
Otherwise, select  $a_t = \text{argmax } \mathcal{Q}^*(s_t, a_t; \alpha, \beta)$ .
- 6:     Perform action  $a_t$  and observe reward  $r_t$  and next state  $s_{t+1}$ .
- 7:     Store transition  $(s_t, a_t, r_t, s_{t+1})$  in the replay memory.
- 8:     Sample random mini-batch of transitions  $(s_j, a_j, r_j, s_{j+1})$  from the replay memory.
- 9:     Combine the value function and advantage functions as follows:

$$\mathcal{Q}(s_j, a_j; \alpha, \beta) = \mathcal{V}(s_j; \beta) + \left( \mathcal{G}(s_j, a_j; \alpha) - \frac{1}{|\mathcal{A}|} \sum_{a_j} \mathcal{G}(s_j, a_j; \alpha) \right). \quad (24)$$

- 10:      $y_j = r_j + \gamma \max_{a_{j+1}} \hat{\mathcal{Q}}(s_{j+1}, a_{j+1}; \alpha^-, \beta^-)$ .
- 11:     Perform a gradient descent step on  $(y_j - \mathcal{Q}(s_j, a_j; \alpha, \beta))^2$ .
- 12:     Every  $C$  steps reset  $\hat{\mathcal{Q}} = \mathcal{Q}$ .
- 13: **end for**

---

deep dueling algorithm for the anti-jamming strategy as shown in Algorithm 2. Note that (23) is viewed and implemented as a part of the network and not as a separated algorithmic step [29]. In addition,  $\mathcal{V}(s; \beta)$  and  $\mathcal{G}(s, a; \alpha)$  are estimated automatically without any extra supervision or modifications in the algorithm.

### B. Complexity Analysis and Implementation

Typically, deep reinforcement learning (and deep learning in general) requires many CPU and GPU resources, especially for large-scale and complex problems which require more hidden layers. Several approaches have been developed to reduce the complexity of deep learning. The authors in [31] proposed the network compression method to convert densely connected neural networks into sparsely connected networks. It was proved that the storage and computation load are reduced by a factor of 10. Moreover, the authors demonstrated that by using the network compression method, deep learning algorithms can be implemented on simple devices such as IoT platforms from Qualcomm, Intel, and NVidia. Note that, our proposed deep dueling algorithm only implements one hidden layer for each stream of the deep neural network. Together with recent advances in network compression, approximate computing, or specialized accelerator hardware, our proposed solution is feasible for general wireless devices.

For ultra-low power IoT devices which cannot implement deep reinforcement learning algorithms, the complex tasks can be offloaded to a nearby resourceful device, e.g., an IoT gateway or a nearby edge computing node. Specifically, at each state  $s_j$ , given the current policy, the transmitter takes an action  $a_j$  and observes the result  $r_j$  and the next state  $s_{j+1}$ . This transition, i.e.,  $(s_j; a_j; r_j; s_{j+1})$ , is then stored in a memory pool. After a certain period, e.g., one hour, the experiences in the memory pool will be sent to a resourceful device to train the deep neural network. Then, the optimal policy, i.e., the Q-table, is sent back to the transmitter to update the current policy. This optimal policy will be then used at the transmitter to make real-time decisions.

## VI. PERFORMANCE EVALUATION

### A. Parameter Setting

In the system under consideration, we set the energy storage capacity at 10 units. The fundamental energy unit can be considered to be  $60 \mu J$  [32]. The data queue of the transmitter can store up to 10 packets in which the packet size can be considered to be 300 bits [33]. The jammer has four transmit power levels, i.e.,  $\mathbf{P}_J = \{0W, 4W, 10W, 15W\}$ , with  $P_{\max} = 15W$  [34]. If the transmitter performs deception and the jammer attacks the channel, the transmitter can harvest energy from or backscatter data through the strong jamming signals. As mentioned, the more power the jammer uses to attack the channel, the more energy and data the transmitter can harvest and backscatter, respectively. Thus, we set  $\mathbf{e} = \{0, 2, 3, 4\}$  and  $\hat{\mathbf{d}} = \{0, 1, 2, 3\}$ . For the rate adaptation technique, we set  $d_m^r = \{2, 1, 0\}$  corresponding to the jamming power levels  $\mathbf{P}_J = \{4W, 10W, 15W\}$ . Other parameters are provided in Table I. Note that our proposed solutions

do not require the information about the jammer and the environment, e.g., data arrival rate, miss detection probability, and backscatter rate, in advance. These information can be learned through the online learning process to obtain the optimal defense policy for the transmitter.

TABLE I: PARAMETER SETTING

| Symbol | $e_v$ | $\hat{d}_a$ | $e_f$ | $\hat{d}_{de}$ | $e_r$ | $p_e$ | $\lambda$ | $K$ | $p_{\text{miss}}$ |
|--------|-------|-------------|-------|----------------|-------|-------|-----------|-----|-------------------|
| Value  | 1     | 4           | 1     | 3              | 1     | 0.5   | 0.7       | 3   | 0.01              |

For deep Q-learning algorithms, for fair comparisons, we adopt parameters based on the common settings for designing neural networks [27], [29]. Specifically, for the deep Q-learning algorithm, two fully-connected hidden layers are implemented together with input and output layers. For the deep dueling algorithm, the neural network is divided into two streams. Each stream consists of a hidden layer connected to the input and output layers as illustrated in Fig. 5. The size of the hidden layers is 64. The mini-batch size is set at 64. The maximum size of the experience replay buffer is 10,000, and the target Q-network is updated every 1,000 iterations [27], [28]. All learning algorithms use the  $\epsilon$ -greedy scheme with the initial value of  $\epsilon$  set at 1 and its final value set at 0.1 [26].

To evaluate the proposed solution, we compare its performance with three other schemes: (i) *harvest-then-transmit (HTT)*, (ii) *backscatter mode (BM)*, (iii) *rate adaptation (RA)*, and (iv) *without deception (WD)*.

- *HTT*: For this policy, the transmitter only implements the harvest-then-transmit (HTT) protocol [18] and uses the harvested energy to actively transmit data, perform the deception, or perform the rate adaptation technique. This scheme is to evaluate the impact of energy harvesting on the system performance.
- *BM*: In this scheme, the transmitter can use the ambient backscatter technique to transmit data or perform the rate adaptation technique when the jammer attacks the channel (after performing deception). This policy evaluates the impact of ambient backscatter communications on the system performance.
- *RA*: With this policy, when the jammer attacks the channel, the transmitter can only perform the rate adaptation technique to transmit data. This scheme is adopted to evaluate the system performance under jamming attacks when the transmitter does not leverage the strong jamming signals.
- *WD*: With this policy, the transmitter will transmit data as long as it has data and sufficient energy. This scheme is used to show the performance of the system without using our proposed deception strategy.

For fair comparisons, the optimal policies of the *HTT*, *BM*, and *RA* schemes are also obtained by the deep dueling algorithm presented in Section V. The performance metrics used for evaluation are the average throughput, packet loss, and packet delivery ratio (PDR). Specifically, the average throughout is defined by the number of packets that the transmitter can successfully transmit to the receiver in a time unit. The packet loss corresponds to the average number of dropped packets in each time unit due to the miss detection, jamming attacks, and limit storage of the data queue. Finally, the PDR is defined by the ratio between the total number of packets arrived at the system and the total number of packets successfully transmitted to the receiver.

### B. Simulation Results

1) *Convergence of Deep Reinforcement Learning Algorithms*: In Fig. 6, we show the convergences of the Q-learning, deep Q-learning, and deep dueling algorithms. It can be observed that, due to the slow-convergence problem, the average throughput obtained by the Q-learning algorithm is much lower than those of the deep Q-learning and deep dueling algorithms. By using the novel deep dueling neural network architecture, the deep dueling can converge to the optimal policy within  $4 \times 10^4$  iterations. For the deep Q-learning algorithm, it cannot obtain the optimal policy after  $10^5$  iterations due to the overestimation of the optimizer. This is due to the overestimation of the optimizer. In contrast, by using the two separated streams to estimate the advantage and value functions, our proposed deep dueling can achieve a faster convergence rate and stable performance. Note that the reactive jammer can adjust its attack policy by sensing the activities on the target channel. Thus, with the proposed deep dueling algorithm, the transmitter can quickly and efficiently adapt the optimal defense strategy when the jammer adjusts its policy. In the next section we use the results obtained by the deep dueling algorithm after  $4 \times 10^4$  iterations and by the Q-learning algorithm after  $10^6$  iterations. Here, the Q-learning algorithm is used as a benchmark to compare the performance with the proposed deep dueling algorithm.

2) *System Performance*: First, we perform simulations to evaluate and compare the utility of the transmitter (under the proposed solution, i.e., Algorithm 2) with that of the jammer. Specifically, the utility of the transmitter is defined by the average number of packets successfully transmitted to the receiver in a time unit, i.e., the average throughput. The utility of the jammer is defined as in Section II-C. It can be observed that, when the average attack power of the jammer increases from 1W to 4W, the average throughput of the proposed solution slightly decreases as the transmitter has less chance to actively transmit data. In addition, harvesting energy from and backscattering data through the jamming signals are not really beneficial when the average attack power of the jammer is low, i.e., less than 4W. When the power budget of the jammer

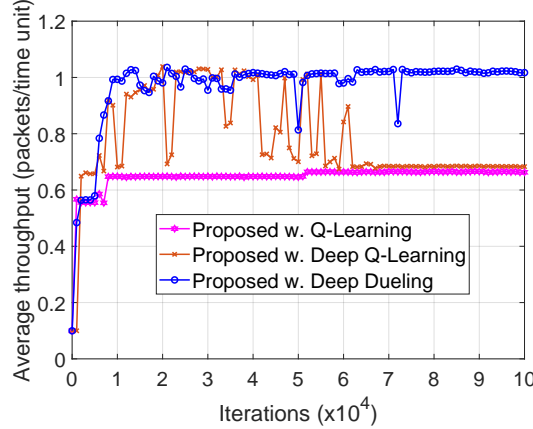


Fig. 6: Convergence rates.

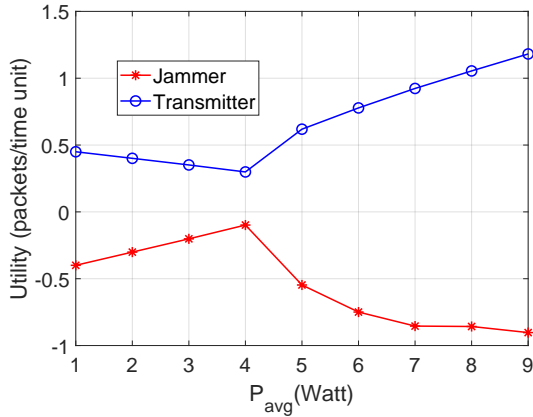


Fig. 7: Utilities of the jammer and the transmitter vs.  $P_{avg}$ .

is larger, i.e.,  $P_{avg} \geq 4W$ , the average throughput obtained by our proposed solution increases as the transmitter has more opportunities to leverage the strong jamming signals to support its transmissions. Thus, the utility of the jammer quickly decreases. This reveals an interesting result that our proposed solution is very effective to deal with reactive jamming attacks even if the jammer has a very high power budget.

Next, we perform simulations to evaluate and compare the performance of our proposed solution with those of the *HTT*, *BM*, *RA*, and *WD* policies in terms of average throughput, packet loss, and packet delivery ratio in several scenarios. In particular, in Fig. 8, we vary the average attack power  $P_{avg}$  of the jammer and observe the performance of the system under different strategies. The performance of the proposed solution can be explained as above. It can be observed that for the *BM*, *HTT* and *RA* strategies, the transmitter only can backscatter data,

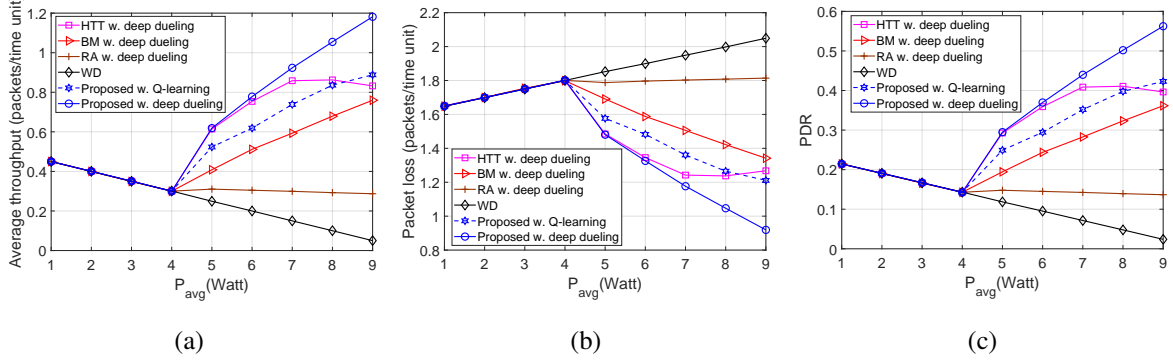


Fig. 8: (a) Average throughput (packets/time unit), (b) Packet loss (packets/time unit), and (c) PDR vs.  $P_{avg}$ .

harvest energy, or reduce the data rate, respectively, under the jamming attack, and thus their performances are much lower than that of the proposed solution which can optimize and trade-off all activities. Note that for the *HTT* policy, the average throughput increases when  $P_{avg}$  increases from 4W to 7W and decreases when the average attack power of the jammer is high. This is due to the fact that when the jammer often attacks the channel, the transmitter has fewer opportunities to actively transmit data to the receiver. For the *WD* policy, the average throughput decreases when the attack probability increases. The reason is that under this policy, the transmitter can only uses the harvested energy from the surrounding environment to actively transmit data when the jammer does not attack the channel. In Fig. 8(b), we show the average number of packet loss of the system. Obviously, the packet loss obtained by our proposed solution is always much lower than those of the other solutions. As a result, the PDR obtained by our proposed solution is higher than those of other solutions as shown in Fig. 8(c).

Next, in Fig. 9, we vary the packet arrival probability and evaluate the system performance in terms of average throughput, packet loss, and PDR under different policies. As shown in Fig. 9(a), when  $\lambda$  increases from 0.1 to 0.6, the average throughput obtained by the proposed deep dueling algorithm increases as the transmitter can transmit more packets. Nevertheless, when  $\lambda > 0.6$ , the average throughput remains stable because the system reaches to the saturation state. Note that the proposed algorithm can always achieve the highest throughput. As such, the PDR obtained by the proposed solution is also higher than those of other schemes as shown in Fig. 9(b). Note that the PDR decreases with  $\lambda$  as the total number of packets arrived in the system increases. Moreover, as shown in Fig. 9(b), the packet loss of the system increases proportionally to the packet arrival rate as the transmitter cannot transmit all the arrival packets and the data queue

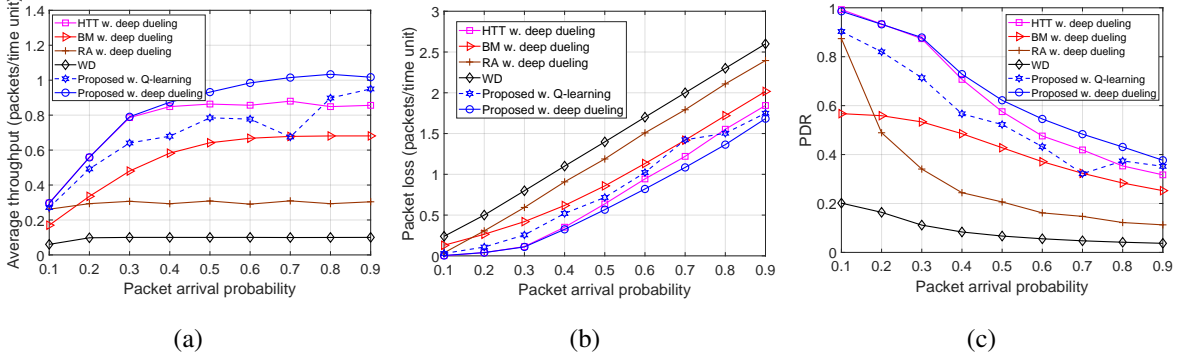


Fig. 9: (a) Average throughput (packets/time unit), (b) Packet loss (packets/time unit), and (c) PDR vs. packet arrival probability.

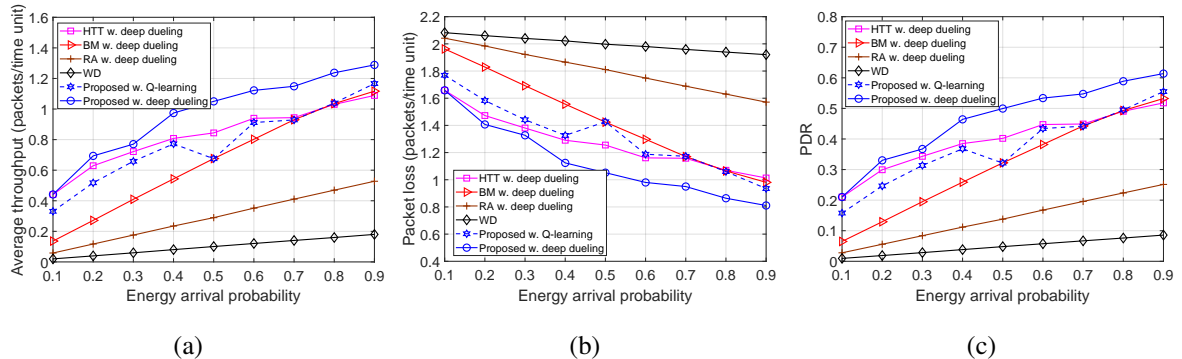


Fig. 10: (a) Average throughput (packets/time unit), (b) Packet loss (packets/time unit), and (c) PDR vs. energy arrival probability.

size is limited. Note that the performance of the Q-learning algorithm is not as good as that of the deep dueling algorithm as it cannot converge to the optimal policy within  $10^6$  iterations.

Finally, we vary the probability that the transmitter can successfully harvest one unit of energy from the environment as shown in Fig. 10. As shown in Fig. 10(a), when  $p_e$  increases, the average throughput of the system obtained by all the solutions increases as the transmitter can harvest more energy from the surrounding environment to support its operations, i.e., deception or active transmissions. This leads to the reduction of the packet loss as shown in Fig. 10(b) and the increase of the PDR in Fig. 10(c). In overall, by optimizing the time for data backscattering, energy harvesting, and rate adaptation, our proposed solution always achieves the highest throughput and lowest packet loss compared to those of the other solutions. Again, the Q-learning algorithm cannot achieve the optimal defense policy for the system due to the slow-convergence problem.

## VII. CONCLUSION

In this paper, we have developed the intelligent anti-jamming framework which allows the transmitter to effectively defeat powerful reactive jamming attacks. Specifically, with the deception mechanism, the transmitter can perform the deception strategy to attract the jammer and drain its power. Furthermore, we introduce the novel ideas of using recent advanced technologies, i.e., ambient backscatter communications and RF energy harvesting, to enable the transmitter to leverage the strong jamming signals while being attacked to further improve system performance. To deal with the dynamic and uncertainty of the jammer and the environment, we have developed the new MDP to formulate the dynamic optimization problem and proposed the deep dueling algorithm to quickly obtain the optimal defense policy for the system. Extensive simulations have demonstrated that the proposed solution can successfully defeat reactive jamming attacks even with very high attack power levels. Interestingly, we have shown that by leveraging the jamming signals, the more frequently the jammer attacks the channel, the greater performance the system can achieve. Moreover, our proposed solution can improve the average throughput by up to 20 times higher compared to the solution without using the deception strategy.

## APPENDIX A THE PROOF OF THEOREM 1

To prove this theorem, we first show that the Markov chain is irreducible. It means that the process can go from one state to any other state after a finite number of steps. In particular, in the system under consideration, the reactive jammer only attacks the channel when the transmitter actively transmits data. Thus, at the beginning of a time slot, the state of the jammer is always idle, i.e.,  $j = 0$ . Similarly, the state of the deception always equals 0 at the beginning of a time slot. As a result, at the beginning of a time slot, the system state is  $s = (0, 0, d, e)$ . If the transmitter chooses to perform the deception and the jammer attacks the channel, the system moves to state  $s' = (1, 1, d, e - e_f)$ . If the jammer does not attack the channel, the system moves to state  $s' = (1, 0, d, e - e_f)$ . Thus, from given states of the jammer and the deception, the system can move to any other states of the jammer and the deception after a finite number of steps.

Similarly, from given data and energy states, the system can move to any other states of the data and energy queues after a finite number of steps. In particular, if the transmitter chooses to actively transmit  $d_a$  packets to the receiver, the the data state moves from  $d$  to  $d - d_a$ , and the energy state moves from  $e$  to  $e - (d_a \times e_r)$ . If the transmitter chooses to perform the deception, the energy state will move from  $e$  to  $e - e_f$ . After performing the deception, if the jammer attacks the channel and the transmitter chooses to harvest energy, the energy state moves from

$e$  to  $e + e_n^J$ . If the transmitter chooses to backscatter data, the data state moves from  $d$  to  $d - d_n^J$ . If the transmitter chooses to adapt its rate, the data state moves from  $d$  to  $d - d_m^r$  and the energy state moves from  $e$  to  $e - (d_m^r \times e_r)$ . In contrast, if the jammer does not attack the channel and the transmitter chooses to actively transmit data, the data state moves from  $d$  to  $d - d_{de}$  and the energy state moves from  $e$  to  $e - (d_{de} \times e_r)$ . If there are  $K$  packets arriving at the system, the data state will move from  $d$  to  $d + K$ . If the transmitter can successfully harvest energy from the ambient RF signals, the energy state moves from  $e$  to  $e + 1$ .

Thus, the state space  $\mathcal{S}$  (which is a combination of the states of the jammer, the deception, the data queue, and the energy queue) contains only one communicating class, i.e., from a given state the process can move to any other states after a finite number of steps. In other words, the MDP with states in  $\mathcal{S}$  is irreducible. As such, the average throughput  $\mathcal{R}(\pi)$  is well defined and does not depend on the initial state for every  $\pi$  [25]. Thus, we can always obtain the optimal policy for the transmitter regardless of the initial system state.

## REFERENCES

- [1] M. K. Hanawal, M. J. Abdel-Rahman, and M. Krunz, "Joint adaptation of frequency hopping and transmission rate for anti-jamming wireless systems," *IEEE Transactions on Mobile Computing*, vol. 15, no. 9, pp. 2247-2259, Sept. 2016.
- [2] A. Mpitsiopoulos, D. Gavalas, C. Konstantopoulos, and G. Pantziou, "A survey on jamming attacks and countermeasures in WSNs," *IEEE Communications Surveys & Tutorials*, vol. 11, no. 4, pp. 42-56, Fourth Quarter 2009.
- [3] W. Xu, K. Ma, W. Trappe, and Y. Zhang, "Jamming sensor networks: attack and defense strategies," *IEEE Network*, vol. 20, no. 3, pp. 41-47, May 2006.
- [4] R. T. Yazicigil, P. Nadeau, D. Richman, C. Juvekar, K. Vaidya, and A. P. Chandrakasan, "Ultra-fast bit-level frequency-hopping transmitter for securing low-power wireless devices," *2018 IEEE Radio Frequency Integrated Circuits Symposium (RFIC)*, PA, USA, Aug. 2018.
- [5] L. Yu, Y. Xu, Q. Wu, and L. Jia, "Self-organizing hit avoidance in distributed frequency hopping multiple access networks," *IEEE Access*, vol. 5, pp. 26614-26622, Nov. 2017.
- [6] H. Quan, H. Zhao, and P. Cui, "Anti-jamming frequency hopping system using multiple hopping patterns," *Wireless Personal Communications*, vol. 81, no. 3, pp. 1159-1176, Apr. 2015.
- [7] A. Mpitsiopoulos, D. Gavalas, G. Pantziou, and C. Konstantopoulos, "Defending wireless sensor networks from jamming attacks," *IEEE PIMRC*, Athens, Greece, Dec. 2007.
- [8] B. Wang, Y. Wu, K. R. Liu, and T. C. Clancy, "An anti-jamming stochastic game for cognitive radio networks," *IEEE Journal on Selected Areas in Communications*, vol. 29, no. 4, pp. 877-889, Apr. 2011.
- [9] Y. Gao, Y. Xiao, M. Wu, M. Xiao, and J. Shao, "Game theory-based anti-jamming strategies for frequency hopping wireless communications," *IEEE Trans. Wireless Commun.*, vol. 17, no. 8, pp. 5314-5326, Aug. 2018.
- [10] Y. Wu, B. Wang, K. R. Liu, and T. C. Clancy, "Anti-jamming games in multi-channel cognitive radio networks," *IEEE Journal on Selected Areas in Communications*, vol. 30, no. 1, pp. 4-15, Jan. 2012.
- [11] K. Pelechrinis, I. Broustis, S. V. Krishnamurthy, and C. Gkantsidis, "Ares: An anti-jamming reinforcement system for 802.11 networks," *ACM CoNEXT*, Rome, Italy, Dec. 2009.
- [12] K. Firouzbakht, G. Noubir, and M. Salehi, "On the capacity of rate-adaptive packetized wireless communication links under jamming," in *Proceedings of the fifth ACM conference on Security and Privacy in Wireless and Mobile Networks*, Tucson, AZ, USA, 2012, pp. 3-14.

- [13] Energy Detection. [Online]. Available: [http://www.dialogic.com/webhelp/msp1010/10.2.3/webhelp/MSP\\_DG/DSP\\_Info/energy\\_detect.htm](http://www.dialogic.com/webhelp/msp1010/10.2.3/webhelp/MSP_DG/DSP_Info/energy_detect.htm)
- [14] G. Noubir, R. Rajaraman, B. Sheng, and B. Thapa, "On the robustness of IEEE 802.11 rate adaptation algorithms against smart jamming," in *Proceedings of the fourth ACM conference on Wireless network security*, Hamburg, Germany, Jun. 2011, pp. 97-108.
- [15] W. Li, J. Wang, L. Li, G. Zhang, Z. Dang, and S. Li, "Intelligent Anti-Jamming Communication with Continuous Action Decision for Ultra-Dense Network," *IEEE ICC*, Shanghai, China, May. 2019.
- [16] J. Guo, N. Zhao, F. R. Yu, X. Liu, and V. CM. Leung, "Exploiting adversarial jamming signals for energy harvesting in interference networks," *IEEE Transactions on Wireless Communications*, vol. 16, no. 2, pp. 1267-1280, Feb. 2017.
- [17] N. V. Huynh, D. N. Nguyen, D. T. Hoang, and E. Dutkiewicz, "Jam Me If You Can: Defeating Jammer with Deep Dueling Neural Network Architecture and Ambient Backscattering Augmented Communications", *IEEE Journal on Selected Areas in Communications*, vol. 37 , no. 11, pp. 2603-2620, Nov. 2019.
- [18] N. V. Huynh, D. T. Hoang, X. Lu, D. Niyato, P. Wang, and D. I. Kim, "Ambient Backscatter Communications: A Contemporary Survey," *IEEE Communications Surveys & Tutorials*, vol. 20 , no. 4, pp. 2889-2922, Fourthquarter 2018.
- [19] C. A. Balanis, *Antenna Theory: Analysis and Design*. New York, NY: Wiley, 2012.
- [20] V. Liu, A. Parks, V. Talla, S. Gollakota, D. Wetherall, and J. R. Smith, "Ambient backscatter: Wireless communication out of thin air," *ACM SIGCOMM*, Hong Kong, China, Aug. 2013.
- [21] C. Boyer and S. Roy, "Backscatter communication and RFID: Coding, energy, and MIMO analysis, *IEEE Transactions on Communications*, vol. 62, no. 3, pp. 770-785, Mar. 2014.
- [22] J. Kimionis, A. Bletsas, and J. N. Sahalos, "Bistatic backscatter radio for tag read-range extension," in *Proceedings of IEEE International Conference on RFID-Technologies and Applications (RFID-TA)*, Nice, France, Nov. 2012, pp. 356-361.
- [23] F. F. Digham, M.-S. Alouini, and M. K. Simon, "On the energy detection of unknown signals over fading channels," *IEEE Transactions on Communications*, vol. 55, no. 1, pp. 21-24, Jan. 2007.
- [24] W. Zhang, R. K. Mallik, and K. B. Letaief, "Optimization of cooperative spectrum sensing with energy detection in cognitive radio networks," *IEEE Transactions on Wireless Communications*, vol. 8, no. 12, pp. 5761-5766, Dec. 2009.
- [25] J. Filar and K. Vrieze, *Competitive Markov Decision Processes*. Springer Press, 1997.
- [26] C. J. C. H. Watkins and P. Dayan, "Q-learning," *Mach. Learn.*, vol. 8, no. 34, pp. 279-292, 1992.
- [27] V. Mnih, K. Kavukcuoglu, D. Silver, A. A. Rusu, J. Veness, M. G. Bellemare, A. Graves, et al., "Human-level control through deep reinforcement learning," *Nature*, vol. 518, no. 7540, pp. 529-533, Feb. 2015.
- [28] I. Goodfellow, Y. Bengio, and A. Courville, *Deep learning*. MIT press, 2016.
- [29] Z. Wang, T. Schaul, M. Hessel, H. V. Hasselt, M. Lanctot, and N. D. Freitas, "Dueling network architectures for deep reinforcement learning," [Online]. Available: [arXiv:1511.06581](https://arxiv.org/abs/1511.06581).
- [30] Dan Sullivan, "Bringing deep learning to IoT devices", [Online]. Available: <https://samsungnext.com/whats-next/deep-learning-iot/>
- [31] S. Han, J. Pool, J. Tran, and W. Dally, "Learning both weights and connections for efficient neural network," in *Proceedings of the 28th International Conference on Neural Information Processing Systems (NIPS)*, Montreal, Canada, Dec. 2015.
- [32] G. Papotto, F. Carrara, A. Finocchiaro, and G. Palmisano, "A 90-nmCMOS 5-Mbps crystal-Less RF-powered transceiver for wireless sensor network nodes," *IEEE Journal of Solid-State Circuits*, vol. 49, no. 2, pp. 335-346, Feb. 2014.
- [33] P. Blasco, D. Gunduz, and M. Dohler, "A learning theoretic approach to energy harvesting communication system optimization," *IEEE Transactions on Wireless Communications*, vol. 12, no. 4, pp. 1872-1882, Apr. 2013.
- [34] 15W Jammer. [Online]. Available: <http://www.jammerall.com/products/Adjustable-6-Antenna-15W-High-Power-WiFi%2CGPS%2CMobile-Phone-Jammer.html>